22. Liou, Y. C. *et al.* Loss of Pin1 function in the mouse resembles the cyclin D1-null phenotypes. *Proc. Natl Acad. Sci. USA* **99,** 1335–1340 (2002).
23. Husseman, J. W., Nochlin, D. & Vincent, I. Mitotic activation: a convergent mechanism for a cohort of neurodegenerative diseases. *Neurobiol. Aging* **21,** 815–828 (2000).
24. Kins, S. *et al.* Reduced protein phosphatase 2A activity induces hyperphosphorylation and altered compartmentalization of tau in transgenic mice. *J. Biol. Chem.* **276,** 38193–38200 (2001).
25. Wolozin, B. L., Pruchnicki, A., Dickson, D. W. & Davies, P. A neuronal antigen in the brains of Alzheimer patients. *Science* **232,** 648–650 (1986).
26. Lee, V. M., Balin, B. J., Otvos, L. Jr & Trojanowski, J. Q. A68: a major subunit of paired helical filaments and derivatized forms of normal Tau. *Science* **251,** 675–678 (1991).
27. Gordon-Krajcer, W., Yang, L. & Ksiezak-Reding, H. Conformation of paired helical filaments blocks dephosphorylation of epitopes shared with fetal tau except Ser199/202 and Ser202/Thr205. *Brain Res.* **856,** 163–175 (2000).
28. Fujimori, F., Takahashi, K., Uchida, C. & Uchida, T. Mice lacking Pin1 develop normally, but are defective in entering cell cycle from G90) arrest. *Biochem. Biophys. Res. Commun* **265,** 658–663 (1999).
29. Patrick, G. N. *et al.* Conversion of p35 to p25 deregulates Cdk5 activity and promotes neurodegeneration. *Nature* **402,** 615–622 (1999).
30. Lucas, J. J. *et al.* Decreased nuclear β-catenin, tau hyperphosphorylation and neurodegeneration in GSK-3β conditional transgenic mice. *EMBO J.* **20,** 27–39 (2001).

Supplementary Information accompanies the paper on **www.nature.com/nature**.

Acknowledgements We thank F. Gage, L. Cantley, B. Neel and K. Kosik for comments on the manuscript; W. Markesbery for human brain samples; P. Davies for tau antibodies; and G. Liu, M. Liu and M. Ericsson for technical assistance. Y.-C.L. is a Fellow of the Canadian Institutes of Health Research, A.R. is a Special Fellow of the Leukemia and Lymphoma Society; T.H. is a Frank and Else Schilling American Cancer Society Research Professor; and K.P.L. is a Pew Scholar and a Leukemia and Lymphoma Society Scholar. This study was supported by NIH grants to G.B., X.J.L., T.H. and K.P.L.

Competing interests statement The authors declare competing financial interests: details accompany the paper on **www.nature.com/nature**.

Correspondence and requests for materials should be addressed to K.P.L. (klu@bidmc.harvard.edu).

Essential role for the peroxiredoxin Prdx1 in erythrocyte antioxidant defence and tumour suppression

Carola A. Neumann[1], Daniela S. Krause[1], Christopher V. Carman[1], Shampa Das[1], Devendra P. Dubey[1], Jennifer L. Abraham[1], Roderick T. Bronson[3], Yuko Fujiwara[2], Stuart H. Orkin[2] & Richard A. Van Etten[1]*

[1]*Center for Blood Research and Department of Genetics, Harvard Medical School, and*
[2]*Howard Hughes Medical Institute, Children's Hospital, Boston, Massachusetts 02115, USA*
[3]*Tufts University School of Veterinary Medicine, North Grafton, Massachusetts 01536, USA*

* Present address: Molecular Oncology Research Institute, Tufts-New England Medical Center, Boston, Massachusetts 02111, USA

Reactive oxygen species are involved in many cellular metabolic and signalling processes[1] and are thought to have a role in disease, particularly in carcinogenesis and ageing[2]. We have generated mice with targeted inactivation of *Prdx1*, a member of the peroxiredoxin family of antioxidant enzymes[3]. Here we show that mice lacking Prdx1 are viable and fertile but have a shortened lifespan owing to the development beginning at about 9 months of severe haemolytic anaemia and several malignant cancers, both of which are also observed at increased frequency in heterozygotes. The haemolytic anaemia is characterized by an increase in erythrocyte reactive oxygen species, leading to protein oxidation, haemoglobin instability, Heinz body formation and decreased erythrocyte lifespan. The malignancies include lymphomas, sarcomas and carcinomas, and are frequently associated with loss of Prdx1 expression in heterozygotes, which suggests that this protein functions as a tumour suppressor. Prdx1-deficient fibroblasts show decreased proliferation and increased sensitivity to oxidative DNA damage, whereas *Prdx1*-null mice have abnormalities in numbers, phenotype and function of natural killer cells. Our results implicate Prdx1 as an important defence against oxidants in ageing mice.

Cellular defences against reactive oxygen species (ROS) include enzymes such as superoxide dismutase (which converts superoxide to hydrogen peroxide), catalase and glutathione peroxidase (which convert hydrogen peroxide to water), as well as non-enzymatic scavengers such as glutathione, ascorbic acid and carotenoids. Peroxiredoxins (Prdxs), a family of small antioxidant proteins that contain essential catalytic cysteine residues and use thioredoxin as an electron donor[3], also scavenge peroxide and are thought to be involved in the cellular response to ROS. Prdxs are abundant proteins found in organisms from all three kingdoms, with at least five distinct members in mammals. Mammalian Prdx1, also known as Pag[4] or MSP23 (ref. 5), is a ubiquitously expressed protein with a relative molecular mass of 23,000 (23K) that is encoded by a single gene on human chromosome 1p34 (ref. 6) and mouse chromosome 4 (ref. 7) and induced by serum stimulation[4] and oxidative stress[5,8]. Transfection studies show that Prdx1 can eliminate peroxide *in vivo* and can regulate ROS induced by growth factor signalling[9]. In addition to its role as an antioxidant enzyme, Prdx1 has been independently isolated as an erythrocyte cytosolic protein that enhances the cytoxicity of natural killer (NK) cells[10], a

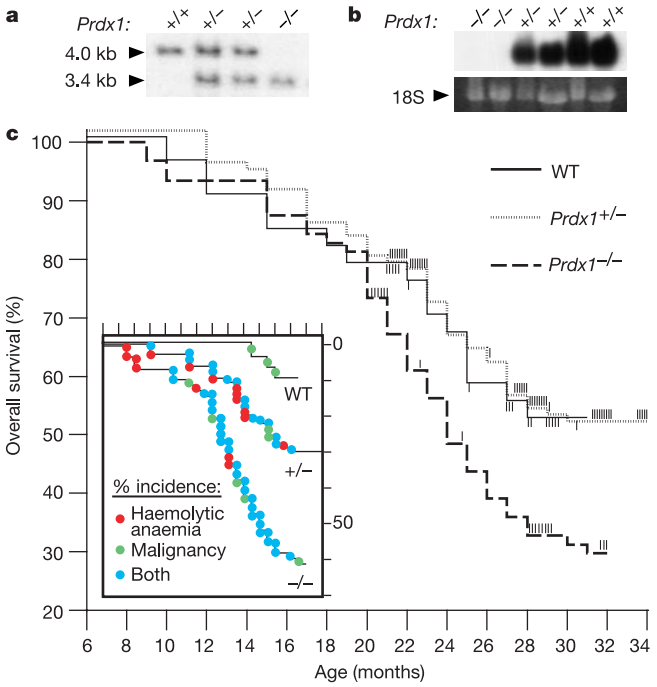

Figure 1 Premature death in ageing *Prdx1* $^{-/-}$ mice. **a**, Genotype of four littermates from a *Prdx1* $^{+/-}$ cross. Southern blot of *Spe*I-digested genomic DNA with a *Prdx1* exon II probe shows wild-type and mutant alleles of 4.0 and 3.4 kilobases, respectively. **b**, Northern blot of total liver RNA from six littermates hybridized with a *Prdx1* complementary DNA probe (top). Ethidium bromide staining of 18S rRNA (bottom) verifies equivalent loading. **c**, Kaplan–Meier survival curve of cohorts of wild-type ($n = 34$), *Prdx1* $^{+/-}$ ($n = 88$) and *Prdx1* $^{-/-}$ ($n = 64$) littermates on a mixed B6 × 129SvEv background. Mutant lines generated from three independently targeted ES cell clones were studied with similar results. The ages of surviving mice are indicated by tick marks. The difference in survival between wild-type and *Prdx1* $^{-/-}$ mice is statistically significant ($P = 0.05$, Mantel–Cox test). Inset, percentage of mice in these cohorts that developed haemolytic anaemia (red), malignancy (green) or both (blue). The *x* axis is identical to the main graph.

Table 1 **Blood parameters of wild-type and anaemic *Prdx1*$^{-/-}$ mice**

	Wild type	*Prdx1*$^{-/-}$
Erythrocytes ($\times 10^6$ per μl)	8.7 ± 0.2	2.4 ± 0.7*
Haematocrit (%)	42.1 ± 2.1	13.1 ± 0.1*
Haemoglobin (g dl^{-1})	13.4 ± 0.5	4.1 ± 0.6*
Erythrocyte volume distribution width (%)	14.2 ± 0.2	24.5 ± 2.0*
Reticulocytes (%)	3.5 ± 2.0	34.0 ± 9.9*
White blood cells ($\times 10^3$ per μl)	8.5 ± 2.7	10.2 ± 9.5
Platelets ($\times 10^3$ per μl)	1,185 ± 169	773 ± 94
Lactate dehydrogenase (U dl^{-1})	270 ± 21	842 ± 229*
Haptoglobin (U dl^{-1})	12 ± 1	<7*
Spleen weight (g)	0.2 ± 0.1	1.0 ± 0.6*

Peripheral blood was obtained from anaemic (defined as haemoglobin < 9) *Prdx1*$^{-/-}$ mice ($n = 8$) and age-matched wild-type littermate controls ($n = 6$). Spleen weights were recorded at autopsy. Values are the mean ± s.e.m.
*For all parameters tested except white blood cells and platelets, the difference between wild-type and *Prdx1*$^{-/-}$ mice was significant ($P < 0.01$, unpaired *t*-test).

cytosolic protein from hepatocytes with high affinity for haem[11], and a cytosolic and nuclear protein that functions as a stoichiometric inhibitor of the non-receptor tyrosine kinase c-Abl[12].

To determine the biological roles of Prdx1, we inactivated the *Prdx1* gene by homologous recombination in murine embryonic stem (ES) cells (Supplementary Fig. 1) and generated heterozygous *Prdx1*$^{+/-}$ mice. In crosses of *Prdx1*$^{+/-}$ mice, *Prdx1*$^{-/-}$ mice were born at the expected mendelian frequency (Fig. 1a and data not shown), lacked *Prdx1* messenger RNA (Fig. 1b), and showed normal postnatal development and fertility. However, prolonged observation of cohorts of wild-type, *Prdx1*$^{-/-}$ and *Prdx1*$^{+/-}$ littermates showed a significantly shortened survival of *Prdx1*$^{-/-}$ mice relative to wild-type littermates (Fig. 1c). Clinicopathological analysis suggested that there were two main causes of premature death in ageing *Prdx1*$^{-/-}$ mice: haemolytic anaemia, which first appeared at 9 months; and malignant tumours. Both diseases were also observed at increased frequency in *Prdx1*$^{+/-}$ mice, beginning at around 12 months, whereas no wild-type mice developed haemolytic anaemia (Fig. 1c, inset).

Many premorbid *Prdx1*$^{-/-}$ mice had severe anaemia characterized by a marked decrease in haematocrit and haemoglobin in peripheral blood relative to wild-type littermate controls, with normal leukocyte and platelet counts (Table 1). Peripheral blood smears from these mice showed prominent microcytosis, anisocytosis, poikilocytosis and polychromatophilia of erythrocytes (Fig. 2a, b), which coincided with an increase in both the width of the erythrocyte volume distribution (Table 1) and the numbers of reticulocytes (Fig. 2c and Table 1). At autopsy, anaemic mice frequently had splenomegaly (Table 1), sometimes massive, owing to extramedullary erythropoiesis (Fig. 2d). These findings are suggestive of anaemia due to decreased survival, rather than impaired production, of erythrocytes. In agreement with this, anaemic mice had increased blood lactate dehydrogenase and decreased haptoglobin (Table 1), indicative of the intravascular destruction of red cells. Similar clinicopathological features were observed in *Prdx1*$^{+/-}$ mice (data not shown), which also developed severe anaemia with age (Fig. 1d).

Serial analysis of blood haemoglobin in the *Prdx1*$^{-/-}$ mice showed a general and gradual decline, which began at around 12 months without any change in reticulocyte numbers (Fig. 2e), similar to wild-type mice (data not shown). However, many ageing *Prdx1*$^{-/-}$ mice showed precipitous drops in blood haemoglobin over an interval of 1–2 months, coincident with and in some mice preceded by an increase in circulating reticulocytes. These data suggest that a subset of *Prdx1*$^{-/-}$ mice develop haemolytic anaemia as they age.

To investigate the cause of the anaemia, we compared the survival of biotin-labelled erythrocytes obtained from anaemic *Prdx1*$^{-/-}$ mice against those from healthy wild-type littermates on transfer into wild-type recipients (Fig. 2f). Whereas the rate of disappearance of labelled wild-type erythrocytes was roughly linear, with a loss of about 2% per day, *Prdx1*$^{-/-}$ erythrocytes disappeared at an exponential rate, indicative of an increase in elimination *in vivo* that was independent of red cell age. These results show that the anaemia

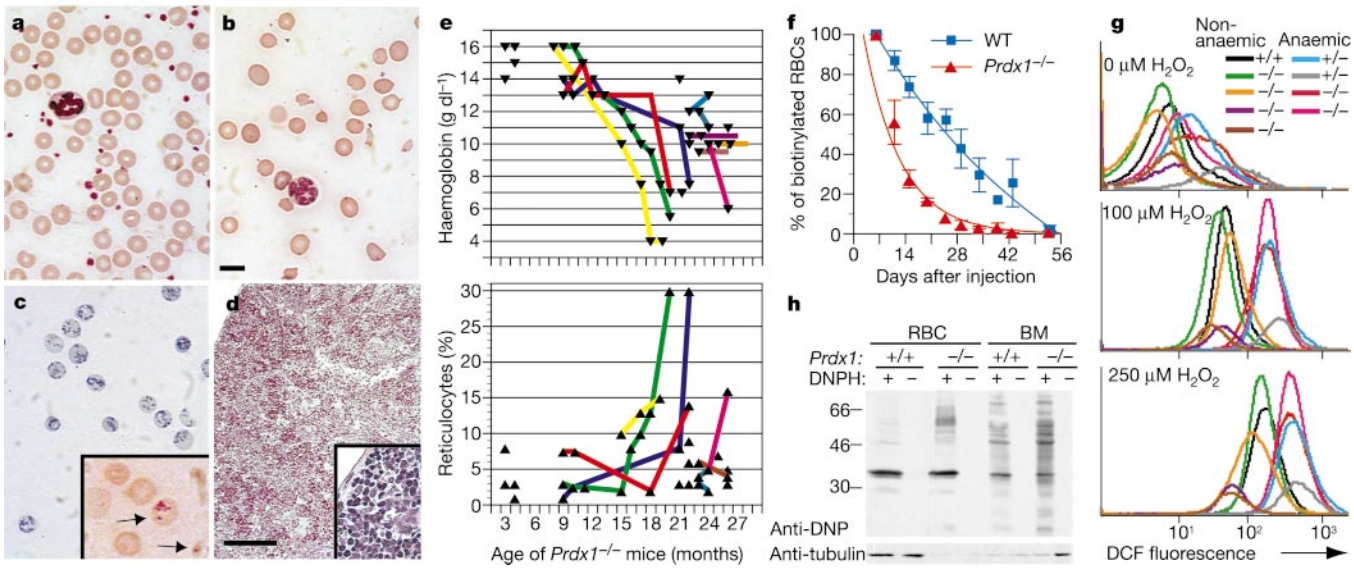

Figure 2 Haemolytic anaemia caused by intra-erythrocytic oxidative damage in *Prdx1* mutant mice. **a**, **b**, Peripheral blood smear (Wright–Giemsa stain) from a healthy wild-type littermate (**a**) and a *Pdrx1*$^{-/-}$ mouse with severe anaemia (**b**). **c**, Peripheral blood (methylene blue stain) from an anaemic *Prdx1*$^{-/-}$ mouse with increased numbers of reticulocytes. Inset, methyl violet stain showing oxidized haemoglobin precipitates (Heinz bodies, arrows). **d**, Spleen (haematoxylin and eosin stain) from an anaemic *Prdx1*$^{-/-}$ mouse, showing disruption of the follicular architecture by extensive extramedullary erythropoiesis (inset). **e**, Blood haemoglobin (top) and reticulocyte counts (bottom) in a subset of *Prdx1*$^{-/-}$ mice plotted against age. Coloured lines link serial values from a single mouse. **f**, Decrease in the intrinsic survival of biotin-labelled erythrocytes from anaemic *Prdx1*$^{-/-}$ mice after adoptive transfer to wild-type recipients. The half-lives were 25 d for wild-type (squares) and 10 d for *Prdx1*$^{-/-}$ (triangles) erythrocytes. Bars indicate the s.e.m. from quadruplicate recipients of the same donor sample; results are representative of two independent experiments. **g**, ROS concentrations measured by DCF fluorescence in erythrocytes from healthy (non-anaemic) wild-type and *Prdx1*$^{-/-}$ mice and from anaemic *Prdx1*$^{+/-}$ and *Prdx1*$^{-/-}$ mice exposed to peroxide *in vitro*. **h**, Protein oxidation in erythrocytes (RBC) and bone marrow cells (BM) from wild-type and anaemic *Prdx1*$^{-/-}$ mice detected by western blotting with an antibody against DNP (top) after treatment with DNPH. After correcting for protein levels (bottom), there was a 6.9-fold and 1.5-fold increase in oxidized proteins in *Prdx1*$^{-/-}$ RBCs and BMs, respectively. Scale bars, 10 μm (**a**–**c**); 100 μm (**d**).

in ageing *Prdx1*$^{-/-}$ mice is due to shortened erythrocyte survival owing to an intrinsic defect in red cells.

The presence of Heinz bodies, representing precipitated haemoglobin, in *Prdx1*$^{-/-}$ erythrocytes (Fig. 2c, inset) suggested that the cause of red cell destruction might be increased erythrocyte ROS, leading to the oxidation of red cell proteins including haemoglobin. In support of this, we observed an increase both in baseline ROS and in ROS generated in response to hydrogen peroxide challenge in erythrocytes from anaemic *Prdx1*$^{-/-}$ and *Prdx1*$^{+/-}$ mice but not in those from age-matched healthy *Prdx1* mutant or wild-type mice (Fig. 2g). Analysis of the carbonyl groups in cellular proteins, a by-product of oxidation, confirmed the increased oxidation of polypeptides in erythrocytes and bone marrow cells of anaemic *Prdx1* mutant mice (Fig. 2h). Finally, we confirmed the presence of oxidized, unstable haemoglobin in erythrocytes from anaemic *Prdx1*$^{-/-}$ mice by showing the increased sensitivity of free haemoglobin in red cell lysates to precipitation by isopropanol (mean precipitated haemoglobin, 33.5 ± 4.3% for *Prdx1*$^{-/-}$ erythrocytes versus 2.1 ± 2.0% for wild type; $P < 0.01$, unpaired *t*-test). Collectively, these results show that ageing *Prdx1* mutant mice develop fatal haemolytic anaemia owing to an increase in erythrocyte ROS, oxidation and precipitation of haemoglobin, and haemolysis.

Cancer was a second main cause of morbidity and death in ageing *Prdx1* mutant mice. Only 3 of 34 wild-type mice died with evidence of malignancy: two from disseminated histiocytic tumours and one from B-cell lymphoma. Both of these cancers are typically found in ageing B6, 129SvEv mice. By contrast, half (32/64) of the *Prdx1*$^{-/-}$ mice succumbed to malignancy either alone or in combination with haemolytic anaemia (Fig. 1d). In addition to B and T lymphomas and histiocytic malignancy, the spectrum of cancers that developed in *Prdx1* mutant mice included epithelial and mesenchymal tumours (hepatocellular carcinoma, fibrosarcoma, osteosarcoma, islet cell adenomas and adenocarcinomas of lung and breast), which are less common in ageing B6, 129SvEv mice (Fig. 3a and Supplementary Fig. 2).

Most sarcomas and lymphomas could be transplanted into nude or sublethally irradiated (275 cGy) severe combined immunodeficient (SCID) mice with latencies of around 1 month or 6 months, respectively (data not shown). An increase in the incidence of malignancy was also observed in *Prdx1*$^{+/-}$ mice (Figs 1d and 3a), although this was not associated with a decrease in overall survival. It is likely that some mice in this cohort had malignancy as a co-morbid condition but died of other causes such as infection. Although the expression of Prdx1 protein was abundant in many normal mouse tissues (Fig. 3b), it was low to undetectable in lysates from several different tumours isolated from *Prdx1*$^{+/-}$ mice (Fig. 3c). This is reminiscent of the inactivation of a tumour suppressor gene and suggests that loss of Prdx1 function may contribute to tumorigenesis. We did not observe any gross structural rearrangements or loss of the wild-type *Prdx1* allele in any tumours from *Prdx1*$^{+/-}$ mice (data not shown), suggesting that either subtle mutations or epigenetic mechanisms such as methylation might be responsible.

To investigate possible mechanisms of tumorigenesis, we characterized murine embryonic fibroblasts (MEFs) derived from *Prdx1*$^{-/-}$ and wild-type littermates. *Prdx1*$^{-/-}$ MEFs proliferated more slowly and had a higher fraction of cells in the G1 phase of the cell cycle than did wild-type MEFs (Fig. 3d). A role for Prdx1 in the cell cycle has been previously suggested because Prdx1 is phosphorylated by Cdc2 during mitosis, resulting in an inhibition of Prdx1 peroxidase activity[13]. The mechanism underlying the slower proliferation of cells lacking Prdx1 is unknown but might reflect chronic oxidative stress. Other studies have shown that overexpressing peroxiredoxins increases cellular resistance to oxidative stress[14,15]. Consistent with this, *Prdx1*$^{-/-}$ MEFs showed signifi-

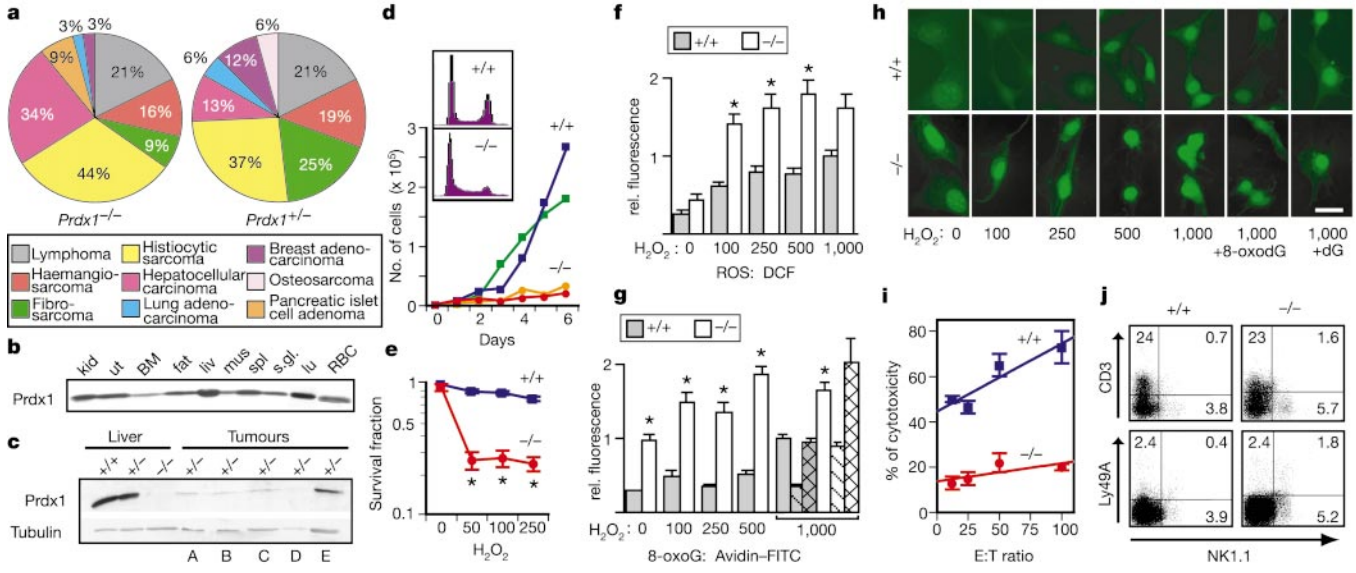

Figure 3 *Prdx1* mutant mice are predisposed to cancer. **a**, Histopathological distribution of tumours observed in *Prdx1*$^{-/-}$ ($n = 32$) and *Prdx1*$^{+/-}$ ($n = 16$) mice. Whereas 38% of tumour-bearing *Prdx1*$^{-/-}$ and *Prdx1*$^{+/-}$ mice had two independent malignancies, 6% of *Prdx1*$^{-/-}$ mice were diagnosed with three different tumours. **b**, Tissue lysates analysed by western blotting with antisera against a GST–Prdx1 fusion protein. **c**, Lysates from normal liver of wild-type, *Prdx1*$^{+/-}$ or *Prdx1*$^{-/-}$ mice (left three lanes) and from independent tumours of *Prdx1*$^{+/-}$ mice (right five lanes: A and B, haemangiosarcoma; C and E, fibrosarcomas; D, osteosarcoma) analysed by western blotting with antibodies against Prdx1 (top) or tubulin (bottom). **d**, Proliferation of *Prdx1*$^{-/-}$ (squares) and wild-type (circles) MEFs. Inset, the fraction of cells with a 2*n* DNA content averaged 44% in wild-type MEFs (top) and 61% in *Prdx1*$^{-/-}$ MEFs (bottom). **e**, Clonogenic survival of *Prdx1*$^{-/-}$ (squares) and wild-type (circles) MEFs after oxidative stress (mean + s.e.m. fractional survival). **f**, Basal and peroxide-induced ROS in *Prdx1*$^{-/-}$ (white bars) and wild-type (grey bars) MEFs, measured by DCF and expressed as the normalized mean + s.e.m. intensity of cell fluorescence. **g**, Basal and peroxide-induced 8-oxoG in *Prdx1*$^{-/-}$ and wild-type MEFs, assessed by staining with avidin-FITC and expressed as in **f**. To show specificity, avidin–FITC was preincubated with an oligonucleotide containing a single 8-oxodeoxyguanosine residue (hatched bars) or a control unoxidized oligonucleotide (crosshatched bars). In **e**–**g**, $^{*}P < 0.001$ (unpaired *t*-test). **h**, Representative photomicrographs of the wild-type and *Prdx1*$^{-/-}$ MEFs shown in **g** treated with the indicated concentration of peroxide and stained with avidin–FITC. Scale bar, 20 μm. **i**, Cytotoxic activity of splenic NK cells from *Prdx1*$^{-/-}$ (circles) and wild-type (squares) mice; bars indicate the s.d. **j**, Frequency of CD3^{+}NK1.1^{+} and NK1.1^{+}Ly49A^{+} cells in enriched splenic NK cell populations from *Prdx1*$^{-/-}$ and wild-type mice.

cantly lower clonogenic survival in response to oxidant treatment (Fig. 3e) and had greater concentrations of peroxide-induced cellular ROS (Fig. 3f) as compared with wild-type MEFs.

We also examined cellular oxidative DNA damage by fluorescence staining of MEFs with fluorescein isothiocyanate (FITC)-conjugated avidin, which detects 8-oxoguanine (8-oxoG)[16]—a principal oxidative DNA lesion that can cause base mispairing and mutations. *Prdx1*$^{-/-}$ MEFs had significantly greater basal and peroxide-induced concentrations of 8-oxoguanine (Fig. 3g) than did wild-type MEFs. The staining was predominantly nuclear (Fig. 3h) and was significantly blocked by preincubating avidin–FITC with an 8-oxoG-containing oligonucleotide but not a non-oxidized oligonucleotide (Fig. 3g, h). Collectively, these observations suggest that loss of Prdx1 increases the susceptibility of non-erythroid tissues to cancer by causing a heightened sensitivity to oxidants and an increase in both cellular ROS and oxidative DNA damage. The loss of Prdx1 protein expression in tumours from *Prdx1*$^{+/-}$ mice is consistent with this mechanism.

Natural killer cells are lymphocyte effector cells of the innate immune system that may be important in protecting against tumour development[17], and Pdrx1 has been identified as an erythrocyte cytosolic protein, NK enhancing factor A (NKEF-A), that stimulates NK activity[10]. We therefore examined NK cells of *Prdx1* mutant mice as another mechanism that might contribute to tumorigenesis. Partially purified splenic NK cells from *Prdx1*$^{-/-}$ mice showed a reproducible and statistically significant decrease in lytic activity towards YAC-1 target cells (Fig. 3i). Flow cytometric analysis detected no significant difference in the frequency of splenic $CD3^{+}NK1.1^{-}$ (19.6 ± 1.9% versus 15.9 ± 3%, respectively) and $CD3^{+}$ $NK1.1^{+}$ cells (0.6 ± 0.2% versus 0.8 ± 0.2%, respectively) between wild-type and *Prdx1*$^{-/-}$ mice; however, an increase (40% to 90%) in the frequency of $CD3^{-}NK1.1^{+}$ cells was observed in all *Prdx1*$^{-/-}$ mice tested (Fig. 3j). A two- to threefold increase in the frequency of a subset of NK cells expressing the inhibitory receptor Ly49A ($NK1.1^{+}Ly49A^{+}$ cells)[18] was also observed in *Prdx1*$^{-/-}$ mice (Fig. 3j). The frequency of NK cells expressing the activation receptor Ly49D[18] was more variable, but in three out of four experiments we observed reduced (<80% of wild-type) frequencies of $NK1.1^{+}Ly49D^{+}$ cells in *Prdx1*$^{-/-}$ mice (data not shown).

We confirmed previous observations that addition of erythrocytes stimulates the cytotoxic activity of NK cells[10], and observed a significant decrease in red blood cell (RBC) NK-enhancing activity when erythrocytes from *Prdx1*$^{-/-}$ mice were added to NK cells from wild-type mice (Table 2). The residual NK-enhancing activity of RBCs lacking Prdx1 could be due to the presence of Prdx2 (also known as NKEF-B), although only Prdx1 shows NK-enhancing activity as a purified protein[19]. Notably, wild-type RBCs had little stimulatory effect on the minimal cytotoxic activity of *Prdx1*$^{-/-}$ NK cells (Table 2), suggesting that Prdx1 may be required in both NK cells and non-immune cells for optimal NK function *in vivo*.

Our results implicate Prdx1 directly in protecting against ROS in red cells and in tumour suppression in ageing mice. Physiological roles for peroxiredoxins in both areas have been postulated[20], but direct proof has been lacking. The main antioxidant defences in red cells were thought to be the glutathione peroxidase and catalase enzyme systems, which use nicotinamide adenine dinucleotide phosphate (NADPH) generated by the hexose monophosphate shunt through glucose 6-phosphate dehydrogenase as the electron donor and glutathione as the direct ROS scavenger. But an absence of either catalase or glutathione peroxidase-1 (ref. 21) does not lead to haemolysis in mice, whereas deficiency of haematopoietic mitochondrial superoxide dismutase causes only mild haemolysis that does not impair survival[22]. By contrast, loss of Prdx1 causes severe fatal haemolytic anaemia but only in ageing mice, which suggests that other red cell antioxidant defences initially compensate for the lack of Prdx1 but that deficiency in these pathways acquired with age leads to haemolysis. Notably, *Prdx1*$^{+/-}$ mice with haemolysis still express Prdx1 in bone marrow or red cells but have about 50% of the Prdx1 concentrations of wild-type mice in these tissues (data not shown), suggesting that large amounts of Prdx1 are necessary for normal red cell survival in older mice.

Similarly, although a role for ROS in carcinogenesis has long been postulated, several mutant mouse strains with deficiencies in antioxidant pathways show an increase in spontaneous cancer development only in response to carcinogens[23,24]. Our results argue that Prdx1 has a direct role in tumour suppression in older mice by eliminating ROS and preventing oxidative DNA damage. Prdx1 and other peroxiredoxins are overexpressed in some human cancers[25], suggesting that tumours that arise through other mechanisms may benefit from increased amounts of peroxiredoxins. Our findings further suggest that Prdx1 regulates NK cell development and cytotoxic function through both cell-autonomous and cell-non-autonomous mechanisms, and that defective NK cell activity may predispose *Prdx1* mutant mice to cancer through a loss of tumour surveillance.

Prdx1 can also inhibit the function of both c-Abl[12] and c-Myc[26], two proteins whose constitutively active forms cause several haematopoietic neoplasms including lymphoma and histiocytic sarcoma. We did not investigate Myc levels or function in *Prdx1*$^{-/-}$ tumours, but several tumours showed an increase in protein tyrosine phosphorylation relative to normal tissues. We did not detect direct tyrosine phosphorylation of c-Abl in these tumours by immunoprecipitation and western blot analysis (data not shown), but this may in part reflect redundancy among the peroxiredoxins, because Prdx3 can also inhibit Abl in transfection experiments (C.A.N. and R.A.V., unpublished data). Establishing the precise mechanisms underlying the cancer susceptibility of *Prdx1* mutant mice will require further studies. These mice should be a valuable tool for understanding the role of antioxidant pathways in ageing, carcinogenesis and other pathophysiological processes.

Note added in proof: Mice deficient in Peroxiredoxin 2 were recently reported to develop nonfatal haemolytic anemia[31]. □

Table 2 **Effects of RBC addition and *Prdx1* genotype on NK cytotoxic activity**

	Fold increase in cytotoxic activity* *Prdx1* genotype of cells				Effector to RBC ratio
NK cells:	+/+	+/+	−/−	−/−	
RBCs:	+/+	−/−	+/+	−/−	
	5.3 ± 1.5†	3.0 ± 1.8	1.2 ± 0.5	1.0 ± 0.5	1:5
	25.6 ± 2.7	16.4 ± 1.7	2.6 ± 0.4	2.9 ± 0.4	1:20

Washed RBCs isolated from wild-type and *Prdx1*$^{-/-}$ mice were mixed with effector cells at two concentrations (RBC to effector ratios of 5 and 20) and a 4-h chromium release assay was done as described[30].

*The effect of RBCs on NK activity is expressed as the fold increase in lytic activity (LA), calculated as (LA in the presence of RBCs – LA in the absence of RBCs)/(LA in the absence of RBCs). RBCs alone did not induce target cell lysis. Values are the mean ± s.e.m.

†Relative to *Prdx1*$^{-/-}$ cells, wild-type NK cells and RBCs showed a 5- and 9-fold increase in lytic activity at RBC to effector ratios of 5 and 20, respectively.

Methods

Generation of *Prdx1*$^{-/-}$ mice

An *Avr*I fragment from a bacterial artificial clone spanning the *Prdx1* locus was cloned into the vector pCWKO. A targeting vector was generated by transposon-mediated mutagenesis[27], in which a transposon carrying unique restriction sites was inserted into exon III of *Prdx1* (Supplementary Fig. 1). We then cloned a *PGK–neo* expression cassette, consisting of the neomycin resistance gene fused to *PGK* promoter, into this vector. ES cells (line Tc-1) were electroporated with this construct and selected for resistance to G418 and gancyclovir. Southern blot analysis showed that 52 of 129 doubly resistant clones analysed were correctly targeted. We injected three independent clones into blastocysts from B6 mice and crossed the resulting chimeras back to B6 mice to generate *Prdx1*$^{+/-}$ mice.

Erythrocyte survival, ROS, protein oxidation and unstable haemoglobin

Erythrocytes from individual healthy wild-type and anaemic *Prdx1*$^{-/-}$ mice were labelled *in vivo* with biotin-X-*N*-hydroxysuccinimide ester (Calbiochem) as described[28], 10^{7} labelled erythrocytes were injected intravenously into wild-type recipient mice, and the kinetics of the disappearance of biotin-labelled cells from circulation was measured by flow cytometric staining with phycoerythrin-conjugated streptavidin.

To measure ROS, we loaded erythrocytes with 10 μM 2′,7′-dichlorodihydrofluorescein diacetate (DCF, Sigma) and analysed intracellular fluorescence intensity by flow cytometry

as described[29]. Protein oxidation in erythroid tissues from anaemic *Prdx1*$^{-/-}$ and age-matched wild-type mice was determined by incubating lysates in the presence or absence of 2,4-dinitrophenylhydrazine (DNPH) to derivatize oxidized carbonyl groups to 2,4-dinitrophenylhydrazone[22], followed by western blotting with an antibody against DNP (Invitrogen). To measure unstable haemoglobin, we lysed erythrocytes from anaemic *Prdx1*$^{-/-}$ ($n = 3$) and age-matched wild-type control ($n = 4$) mice with distilled water and precipitated the membranes by adding 150 mM NaCl. The supernatant was analysed for haemoglobin concentration before and after the addition of 17% isopropanol by spectrophotometric determination of absorbance at 540–580 nm.

Cell cycle, clonogenic survival, ROS and 8-oxoG analysis

MEFs established from two independent pairs of wild-type and *Prdx1*$^{-/-}$ littermates were plated in duplicate cultures and the cell number was determined daily. We analysed the DNA content by flow cytometric analysis using propidium iodide staining of unsynchronized cells collected on day 4. To assess clonogenic survival in response to oxidative stress, MEFs were treated with hydrogen peroxide for 30 min and plated in triplicate, and the colonies were counted 7 d later.

To measure ROS concentrations, MEFs were stimulated with peroxide for 10 min in serum- and phenol-red-free medium, incubated with 50 μM DCF for 10 min, and then washed and analysed with a Axiovert S200 microscope (Zeiss) and an Ocra CCD (charge-coupled device) camera (Hamamatsu). At least 15 individual cell images were acquired per condition, background levels were subtracted, and the mean total cellular fluorescence intensity was quantified by OpenLab 3.1.2 software (Improvision). Results are expressed as the mean fluorescence intensity normalized to that of wild-type cells treated with 1,000 μM peroxide.

To measure 8-oxoG, MEFs growing on fibronectin-coated coverslips were treated with peroxide in serum-free and phenol-red-free medium for 2 h at 37 °C, fixed in absolute methanol (−20 °C, 20 min) and permeabilized with 0.1% Triton X-100 (room temperature, 15 min). After nonspecific binding sites were blocked, the cells were stained with 15 μg ml^{-1} FITC-conjugated avidin (Sigma) for 1 h at 37 °C. To verify specificity of the detection of 8-oxoG, avidin-FITC was preincubated with an eightfold excess of either a 23-base oligodeoxynucleotide (Sigma) containing a single 8-oxodeoxyguanosine residue or a control unoxidized oligonucleotide. We measured and quantified the normalized the mean cellular fluorescence intensity as described above.

NK cell cytolytic activity and cell-surface antigen expression

Splenocytes from *Prdx1*$^{-/-}$ ($n = 15$) and age-matched wild-type ($n = 15$) young mice were enriched for NK cells by centrifugation over Lympholyte-M (Cedarlane Laboratories) and passage over a nylon wool column. We determined cytotoxic activity in duplicate at four different effector to target ratios in a 4-h chromium-release assay by using ^{51}Cr-labelled YAC-1 cells as a target as described[30]. Specific cytotoxicity was calculated as the percentage of specific cytotoxicity = [c.p.m.(ER) − c.p.m.(SR)]/[c.p.m.(MR)–c.p.m.(SR)] × 100, where ER is the ^{51}Cr release in experimental wells, SR is the spontaneous ^{51}Cr release, and MR is the maximum ^{51}Cr release in the presence of 10% SDS. Cytotoxic activity was expressed in lytic activity units (LA) per 10^6 cells, which is defined as the number of effector cells required for 20% lysis of the labelled target cells. The specific cytotoxic activity of wild-type and *Prdx1*$^{-/-}$ NK cells was 91 and 3.6 LA per 10^6 cells, respectively. Enriched splenic NK cell populations from wild-type and *Prdx1*$^{-/-}$ mice were analysed by flow cytometry with directly conjugated monoclonal antibodies against CD3, NK1.1, Ly49A and Ly49D (PharMingen).

Received 14 February; accepted 27 May 2003; doi:10.1038/nature01819.

1. Finkel, T. Oxygen radicals and signaling. *Curr. Opin. Cell Biol.* **10,** 248–253 (1998).
2. Finkel, T. & Holbrook, N. J. Oxidants, oxidative stress and the biology of ageing. *Nature* **408,** 239–246 (2000).
3. Chae, H. Z. *et al.* Cloning and sequencing of thiol-specific antioxidant from mammalian brain: alkyl hydroperoxide reductase and thiol-specific antioxidant define a large family of antioxidant enzymes. *Proc. Natl Acad. Sci.* **91,** 7017–7021 (1994).
4. Prosperi, M. T., Ferbus, D., Karczinski, I. & Goubin, G. A human cDNA corresponding to a gene overexpressed during cell proliferation encodes a product sharing homology with amoebic and bacterial proteins. *J. Biol. Chem.* **268,** 11050–11056 (1993).
5. Ishii, T. *et al.* Cloning and characterization of a 23-kDa stress-induced mouse peritoneal macrophage protein. *J. Biol. Chem.* **268,** 18633–18636 (1993).
6. Prosperi, M. T., Apiou, F., Dutrillaux, B. & Goubin, G. Organization and chromosomal assignment of two human PAG gene loci: PAGA encoding a functional gene and PAGB a processed pseudogene. *Genomics* **19,** 236–241 (1994).
7. Lyu, M. S. *et al.* Genetic mapping of six mouse peroxiredoxin genes and fourteen peroxiredoxin related sequences. *Mammal. Genome* **10,** 1017–1019 (1999).
8. Prosperi, M.-T., Ferbus, D., Rouillard, D. & Goubin, G. The *pag* gene product, a physiological inhibitor of c-*abl* tyrosine kinase, is overexpressed in cells entering S phase and by contact with agents inducing oxidative stress. *FEBS Lett.* **423,** 39–44 (1998).
9. Kang, S. W. *et al.* Mammalian peroxiredoxin isoforms can reduce hydrogen peroxide in response to growth factors and tumor necrosis factor-α. *J. Biol. Chem.* **273,** 6297–6302 (1998).
10. Shau, H., Gupta, R. K. & Golub, S. H. Identification of a natural killer enhancing factor (NKEF) from human erythroid cells. *Cell. Immunol.* **147,** 1–11 (1993).
11. Iwahara, S. *et al.* Purification, characterization, and cloning of a heme-binding protein (23 kDa) in rat liver cytosol. *Biochemistry* **34,** 13398–13406 (1995).
12. Wen, S.-T. & Van Etten, R. A. The *PAG* gene product, a stress-induced protein with antioxidant properties, is an Abl SH3-binding protein and a physiological inhibitor of c-Abl tyrosine kinase activity. *Genes Dev.* **11,** 2456–2467 (1997).
13. Chang, T.-S. *et al.* Regulation of peroxiredoxin I activity by Cdc2-mediated phosphorylation. *J. Biol. Chem.* **277,** 25370–25376 (2002).
14. Shau, H. *et al.* Endogenous natural killer enhancing factor-B increases cellular resistance to oxidative stress. *Free Radic. Biol. Med.* **22,** 497–507 (1997).
15. Chung, Y. M., Yoo, Y. D., Park, J. K., Kiim, Y.-T. & Kim, H. J. Increased expression of peroxiredoxin II confers resistance to cisplatin. *Anticancer Res.* **21,** 1129–1134 (2001).
16. Struthers, L., Patel, R., Clark, J. & Thomas, S. Direct detection of 8-oxodeoxyguanosine and 8-oxoguanine by avidin and its analogues. *Anal. Biochem.* **255,** 20–31 (1998).
17. Cerewenka, A. & Lanier, L. L. Natural killer cells, viruses and cancer. *Nature Rev. Immunol.* **1,** 41–49 (2001).
18. Takei, F., Brennan, J. & Mager, D. L. The Ly49 family: genes, proteins and recognition of class I MHC. *Immunol. Rev.* **155,** 67–77 (1997).
19. Sauri, H., Ashjian, P. H., Kim, A. T. & Shau, H. Recombinant natural killer enhancing factor augments natural killer cytotoxicity. *J. Leuk. Biol.* **59,** 925–931 (1996).
20. Butterfield, L. H., Merino, A., Golub, S. H. & Shau, H. From cytoprotection to tumor suppression: the multifactorial role of peroxiredoxins. *Antioxid. Redox Signal.* **1,** 385–402 (1999).
21. Johnson, R. M., Goyette, G., Ravindranath, Y. & Ho, Y.-S. Red cells from glutathione peroxidase-1-deficient mice have nearly normal defenses against exogenous peroxides. *Blood* **96,** 1985–1988 (2000).
22. Friedman, J. S. *et al.* Absence of mitochondrial superoxide dismutase results in a murine hemolytic anemia responsive to therapy with a catalytic antioxidant. *J. Exp. Med.* **193,** 925–934 (2001).
23. Henderson, C. J. *et al.* Increased skin tumorigenesis in mice lacking pi class glutathione S-transferases. *Proc. Natl Acad. Sci. USA* **95,** 5275–5280 (1998).
24. Ramos-Gomez, M. *et al.* Sensitivity to carcinogenesis in increased and chemoprotective efficacy of enzyme inducers is lost in Nrf2 transcription factor-deficient mice. *Proc. Natl Acad. Sci. USA* **98,** 2941–2943 (2001).
25. Noh, D.-Y. *et al.* Overexpression of peroxiredoxin in human breast cancer. *Anticancer Res.* **21,** 2085–2090 (2001).
26. Mu, Z. M., Yin, X. Y. & Prochownik, E. V. Pag, a putative tumor suppressor, interacts with the Myc box II domain of c-Myc and selectively alters its biological function and target gene expression. *J. Biol. Chem.* **277,** 43175–43184 (2002).
27. Westphal, C. H. & Leder, P. Transposon-generated 'knock-out' and 'knock-in' gene-targeting constructs for use in mice. *Curr. Biol.* **7,** 530–533 (1997).
28. Hoffmann-Fezer, G. *et al.* Biotin labeling as an alternative nonradioactive approach to determination of red cell survival. *Ann. Hematol.* **67,** 81–87 (1993).
29. Frank, J., Biesalski, H. K., Dominici, S. & Pompella, A. The visualization of oxidant stress in tissues and isolated cells. *Histol. Histopathol.* **15,** 173–184 (2000).
30. Dubey, D. P. *et al.* The MHC influences NK and NKT cell functions associated with immune abnormalities and life span. *Mech. Aging Dev.* **113,** 117–134 (2000).
31. Lee, T.-H. *et al.* Peroxiredoxin II is essential for sustaining life span of erythrocytes in mice. *Blood* **101,** 5033–5038 (2003).

Supplementary Information accompanies the paper on **www.nature.com/nature**.

Acknowledgements We thank C. Westphal, P. Leder, K. Smith, J. Alverez, J. Pinkas and C. Brugnara for assistance, and H. F. Bunn for discussions. This work was supported by NIH grants to C.A.N., S.D., D.P.D. and R.A.V.

Competing interests statement The authors declare that they have no competing financial interests.

Correspondence and requests for materials should be addressed to R.A.V. (rvanetten@tufts-nemc.org).

Machinery for protein sorting and assembly in the mitochondrial outer membrane

Nils Wiedemann[1,2], Vera Kozjak[1,2], Agnieszka Chacinska[1], Birgit Schönfisch[1], Sabine Rospert[3], Michael T. Ryan[1]*, Nikolaus Pfanner[1] & Chris Meisinger[1]

[1]*Institut für Biochemie und Molekularbiologie, Universität Freiburg, Hermann-Herder-Str. 7, D-79104 Freiburg, Germany*
[2]*Fakultät für Biologie, Universität Freiburg, D-79104 Freiburg, Germany*
[3]*Max-Planck Research Unit Enzymology of Protein Folding, Weinbergweg 22, D-06120 Halle, Saale, Germany*

* Present address: Department of Biochemistry, La Trobe University, 3086 Melbourne, Australia

Mitochondria contain translocases for the transport of precursor proteins across their outer and inner membranes[1–5]. It has been assumed that the translocases also mediate the sorting of proteins to their submitochondrial destination[1,2,5–10]. Here we show that the mitochondrial outer membrane contains a separate sorting and assembly machinery (SAM) that operates after the